

International Atomic Energy Agency

INDC(CHL)-003/L

INDC

INTERNATIONAL NUCLEAR DATA COMMITTEE

TOTAL NEUTRON CROSS SECTIONS AT ENERGIES AROUND 20 MeV

J.R. Morales, J.L. Romero, and P. Martens

September 1990

IAEA NUCLEAR DATA SECTION, WAGRAMERSTRASSE 5, A-1400 VIENNA

TOTAL NEUTRON CROSS SECTIONS AT ENERGIES AROUND 20 MeV

J.R. Morales, J.L. Romero, and P. Martens

September 1990

**Reproduced by the IAEA in Austria
September 1990**

90-04596

TOTAL NEUTRON CROSS SECTIONS AT ENERGIES AROUND 20 MeV

J. R. Morales*, J. L. Romero#, and P. Martens&

The results for measurements of total cross sections on C, Al, Mg, Cu, Ge and Pb at 17.6 and 19.8 MeV are reported. A detailed comparison is presented with previous data and with the global optical model by the Ohio group. We also discuss plans for total non elastic cross section measurements.

Introduction

At the Nuclear Physics Laboratory of the University of Chile, a facility for fast neutron research in the energy range from 15 to 22 MeV has been designed. Here, neutrons are generated with the $d + T$ reaction using deuteron beams provided by the 56 cm isochronous cyclotron, with variable energies up to 5 MeV.

Among other possibilities, the measurement of total non-elastic cross sections have been planned considering the request of this kind of neutron data ^[1,2] and the overall capability of this laboratory to accomplish it. In order to extract the total non-elastic values, the knowledge of the total cross section at the same energies is required. Therefore, as a first step we have performed a series of total cross section measurements at two energies, 17.6 and 19.8 MeV. Additionally, this experiment allowed us to test many experimental conditions such as beam stability, time of flight techniques, detectors efficiencies, etc. Here we describe the facility and present the total cross section values obtained for these energies.

Experimental

Deuterium ions are produced and accelerated by an isochronous cyclotron of variable energy. Neutrons are then produced by the reaction ${}^3\text{H}(d,n){}^4\text{He}$. Description and main characteristics of this accelerator are given elsewhere.^[3] Once the deuterons have acquired the desired energy they are extracted and sent to the neutron pit, distant about 10 m from the cyclotron vault as shown in the layout, fig. 1 .

The neutron pit was designed for fast neutron research, being almost spherical in shape with a radius of 5 m and 1 m concrete walls. In order to retard detection of bounced neutrons

*Departamento de Física, Facultad de Ciencias, Universidad de Chile, Santiago, Chile

#Crocker Nuclear Laboratory and Department of Physics, University of California, Davis, California, U.S.A.

&Departamento de Física, Facultad de Ciencias Físicas y Matemáticas, Universidad de Chile, Santiago, Chile

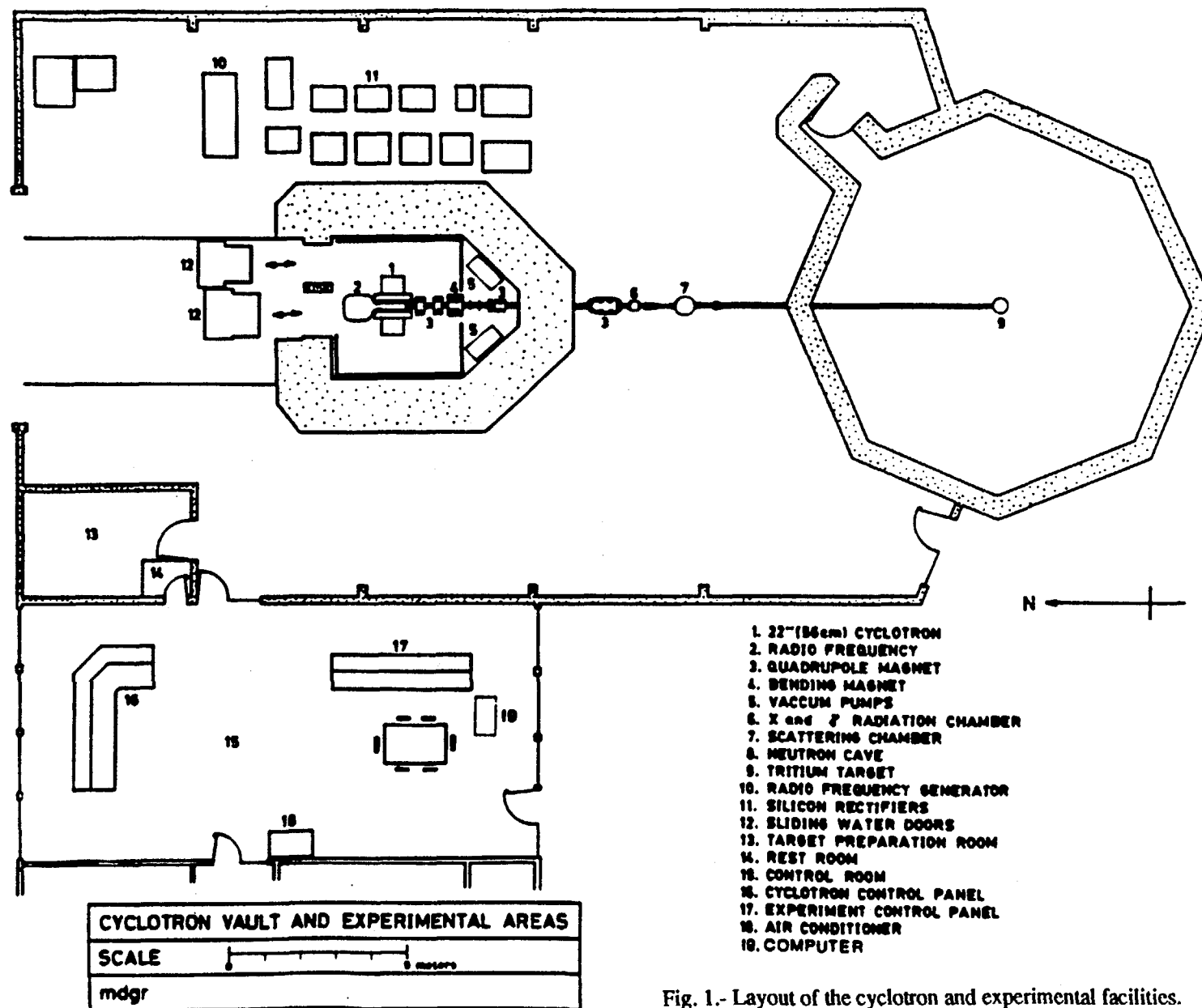


Fig. 1.- Layout of the cyclotron and experimental facilities.

from the walls, ceiling and floor, the neutron target is located at the center of the room. The floor is made of light material, wood, properly reinforced at points where heavy equipment is installed. In order to obtain monoenergetic neutrons, extremely thin titanium-tritium films deposited on platinum foil backings of 70 μm are used. An aluminum ring provides necessary support and strength. These targets, provided by a grant of INDC, IAEA, were manufactured by Metronex, Warzav, and their initial activity was 20 Ci, with a tritium to titanium ratio of 1.99. The net tritium target area covers a disc of about 20 mm in diameter. The target set-up and cooling is similar to the one described previously.^[4] The backing materials used in this type of targets imply that other reactions involving deuterons on Ti and Pt may produce fast neutrons too, such as $^{48}\text{Ti}(d,n)^{49}\text{V}$ and $^{195}\text{Pt}(d,n)^{196}\text{Au}$. Due to the much lower Q-values of these reactions, +4.54 MeV and +3.44 MeV respectively, their expected neutrons can be separated by time of flight (TOF) from those originated in the main reaction.

In this experiment a deuteron beam of 3.41 MeV was used. The beam intensity was restricted to about 1 μA in order to avoid overheating of the target. A set of lead and tantalum collimators plus quadrupole magnetic lenses concentrate the deuteron beam at the center of the target. The beam intensity was not significantly affected by its path through the target, and therefore a Faraday cup located behind the target at 15 cm permitted a constant deuteron beam monitoring.

A movable arm centered at the tritium target was designed to hold a neutron collimator, two neutron detectors and the sample target holder. The arm can rotate in the horizontal plane allowing a kinematic selection of neutrons. Rotation is possible from 0° to 90° , sweeping a neutron energy range from 20.1 MeV to 15.4 MeV for an incident deuteron beam of 3.41 MeV. This set-up is shown in fig. 2. Neutrons emitted from the T-Ti target are selected by an iron collimator 31 cm long and with a square aperture of 1 cm^2 .

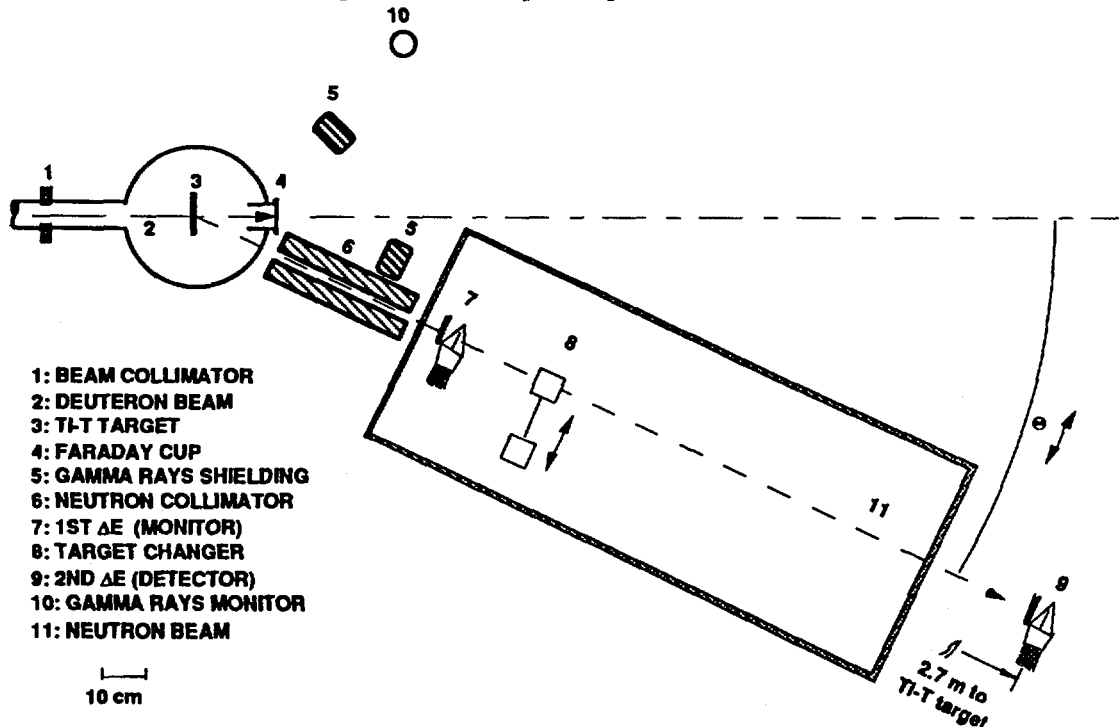


Fig. 2.- Neutron production area and experimental set-up for the total cross section measurements.

The energy of the deuteron beam was determined by standard procedures and independently verified by the measurement of the neutron energy by time of flight. A value of 3.41 +/- 0.08 MeV was obtained.

Close to the iron collimator and at 61 cm from the Ti-T target the first neutron detector was located while the second detector was at 277 cm (fig. 2). In between both detectors, and at 20 cm from the first one a sample target holder was installed. The holder has the capability of moving the target back and forth from the neutron path by remote control. In this way measurements with target in and out were done without alteration of beam conditions. Additional shielding was provided to protect detectors from gamma rays originated at the Faraday cup and collimators.

Six targets made of different elements were used in this experiment. Their purity was checked by PIXE at the same laboratory finding total impurities below 0.3 %. In the case of carbon, where PIXE is not applied, the purity is credited to manufacturer which gives a lower value of 99 % for this reactor quality graphite. All targets were given cylindrical shapes with lengths chosen to allow a 80 % transmission for 20 MeV neutrons, and with areas larger than the neutron beam cross section. Characteristics of the targets are given in Table I.

TABLE I. Targets characteristics.

Element	Nuclei density $10^{22}/\text{cm}^2$	Length cm	Area cm^2	Purity %
C	11.3	3.00	4.95	99.0
Mg	4.30	3.02	5.11	99.7
Al	6.01	2.54	5.01	99.7
Cu	8.46	1.50	5.07	99.7
Ge	4.40	2.64	6.84	99.7
Pb	3.30	2.00	6.25	99.7

As shown in fig. 2, two neutron detectors were used to determine the number of neutrons coming from the Ti-T target through the iron collimator. They have been labeled ΔE_1 and ΔE_2 and are of similar material and dimensions. Each one consists of a rectangular sheet of plastic scintillator NE-102 of 0.8 mm in thickness and $35.8 \times 58.7 \text{ mm}^2$ in area, attached to a Lucite light-guide which rests on the surface of a 8575 RCA photomultiplier tube (see fig. 3). The neutron to proton converter was a 2 mm paraffin sheet [hydrogen to carbon ratio slightly better than polyethylene (CH_2)] preceded by a 2 mm graphite sheet that acted as a charged particle "veto" (this graphite sheet will stop a 20 MeV proton). The low energy protons produced by the $^{12}\text{C}(n,p)$ reaction (Q-value is -12.59 MeV) can be considered as a contribution to the efficiency of the converter.

The dimensions of the paraffin converter and of the NE-102 scintillating material were carefully chosen such that signals induced by full energy neutrons have a small variation range. In fig. 3, we illustrate the case of 20 MeV neutrons striking on the converter and producing protons through the H(n,p) reaction at angles and places as shown. Protons lose some amount of energy in the scintillator, which is 1.3 MeV for trajectory *a*, 1.7 MeV for trajectories *b* and *c* and 2.5 MeV for trajectory *d*. This allows us to set the discriminator threshold at 1 MeV protons, which is equivalent to about 10 MeV electrons, thus establishing a plateau region .

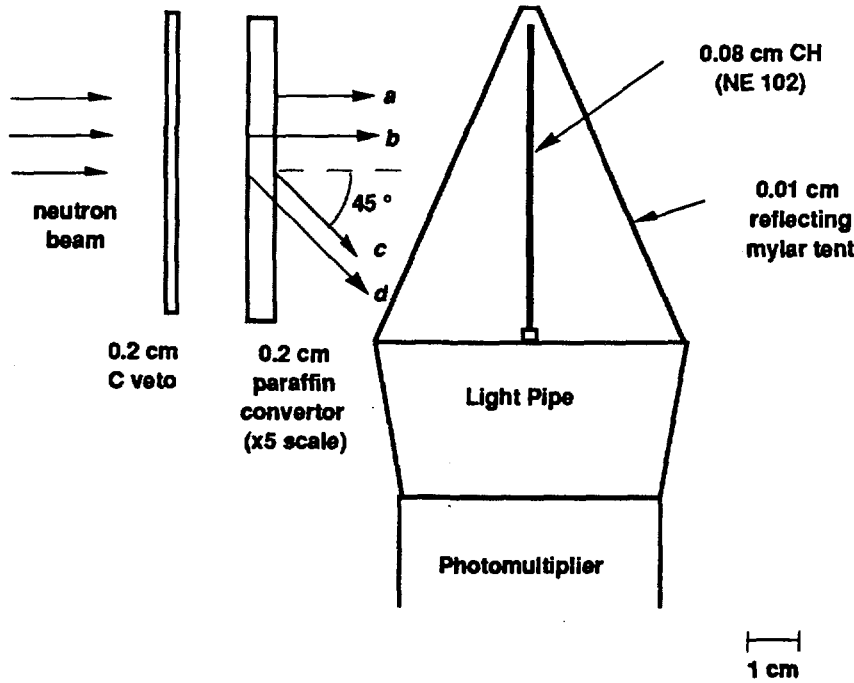


Fig. 3.- Side view of the ΔE detector showing some critical proton trajectories .

An important consideration related with the detection of fast neutrons using TOF in cyclic accelerators, deals with the probable contamination of neutrons of lower energy for which the combinations of distance and energy give a TOF just one radiofrequency (rf) period less than that of the (higher energy) neutrons of interest. These neutrons -if above the detector threshold- cannot be distinguished from the main neutrons in a TOF measurement. This group of neutrons will be called the "wrap around neutrons". In this experiment such contamination was produced and its contribution evaluated and discussed below .

In general, the wrap around neutrons satisfy the time relationship

$$t_w = t_o + T,$$

where t_o is the TOF of neutrons of energy E , t_w is the TOF of wrap around neutrons of energy E_w , and T is the rf period. For non relativistic neutrons, we can express the above equation in terms of the energies as

$$\frac{1}{\sqrt{E_w}} = \frac{1}{\sqrt{E_o}} + \frac{T}{72.3 \text{ d}} \quad (1)$$

where d is the distance from the Ti-T target to detectors, in meters, T is in nsec, and the energies are in MeV.

Fig. 4 is a plot of E_w vs distance for $T=43.1$ nsec and $E=21$ MeV neutrons. One can see that for a distance of 0.6 m, corresponding to the actual position of ΔE_1 (fig. 2), the energy for the wrap around neutrons is 0.7 MeV. Instead, for $d=2.7$ m, $E_w=5.2$ MeV. Then, since the thresholds of our detectors were set at 1 MeV, only detector ΔE_2 was sensitive to wrap around neutrons. A correction for this effect is given later.

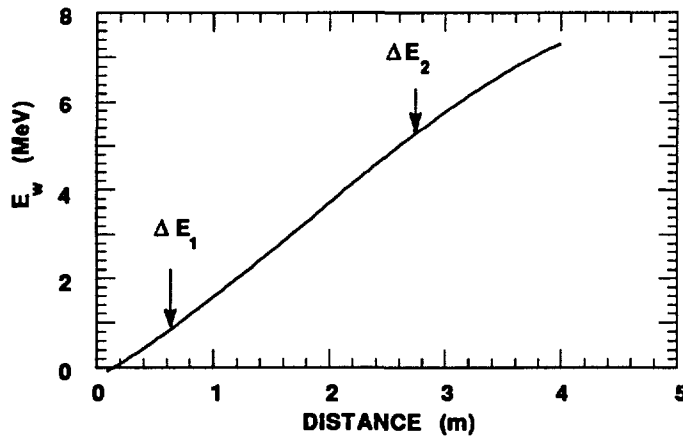


Fig. 4.- Energy of wrap around neutrons vs distance between the neutron producing target and detector, corresponding to 21 MeV neutrons and to a radiofrequency period of 43.1 nsec. Shown are the positions of the detectors.

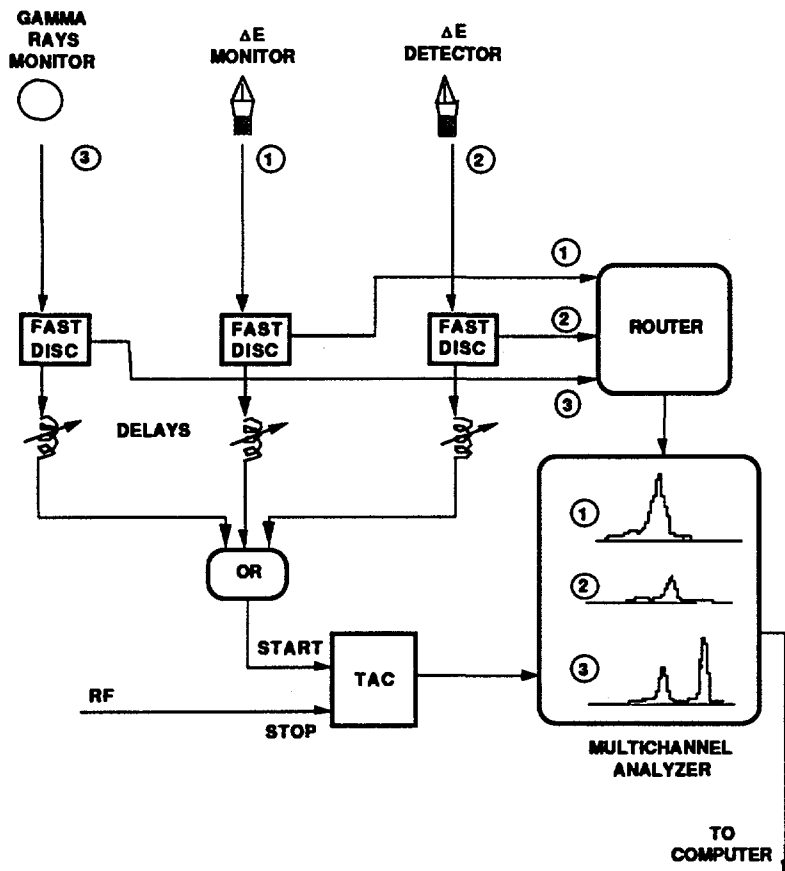


Fig. 5.- Block diagram of the electronics for the total cross section measurements.

A third detector was a 5.04 cm height by 5.04 cm in diameter NE-102 plastic cylinder. This detector was used to monitor the gamma flash from the target . The TOF spectrum is very sensitive to time shifts in the beam relative to the rf. [5]

Only fast electronics was used during data acquisition, since the only parameter measured was TOF relative to the rf. Fig. 5 is a block diagram of the electronics. We used a fairly stable deuteron beam of 3.4 MeV, which corresponds to a rf period of 43.1 nsec. However, analog signals were available to set the thresholds.

The main feature of the electronics setup was that a common time to amplitude (TAC) converter was used for the three detectors, and a route system allowed to store the corresponding TOF spectrum simultaneously (fig. 5). The advantage of this scheme is that rf shifts could be corrected for by comparing the spectrum from ΔE_1 and ΔE_2 with that observed in the cylindrical monitor.

Measurement.

The measurement of the total cross section is based on the comparison of neutron fluxes in two different cases : at air and when a particular target intercepts the neutron beam. Then

$$\sigma = \frac{1}{NL} \ln \frac{\left[\frac{I_2}{I_1} \right]_{out}}{\left[\frac{I_2}{I_1} \right]_{in}} ,$$

which is independent of the detector efficiencies, and I_1 and I_2 are the measured incident and transmitted beam intensities, respectively.

The experimental problem consists now in the measurement of neutron rates. By allowing simultaneous operation of the detectors ΔE_1 and ΔE_2 , the intensity ratios are equal to the ratios of the number of the neutrons detected at each detector, or

$$\frac{\left[\frac{I_2}{I_1} \right]_{out}}{\left[\frac{I_2}{I_1} \right]_{in}} = \frac{\left[\frac{n_2}{n_1} \right]_{out}}{\left[\frac{n_2}{n_1} \right]_{in}} .$$

In this experiment the number of neutrons was determined with the system described previously. In fig. 6 neutron spectra from detectors ΔE_1 and ΔE_2 are shown for target in (full line) and target out (dotted line).

Several corrections were considered, most of them are eliminated by the ratio involving target in and out. One that remains in our experiment is due to the low energy wrap around neutrons, LEN. The origin of the LEN is in nuclear reactions between deuterons and the backing materials of the tritium target. In our case, there are two different elements to consider, titanium and platinum, with (d,n) Q-values between 2.90 and 5.83 MeV. A second source of LEN is in the lead in the Faraday cup.

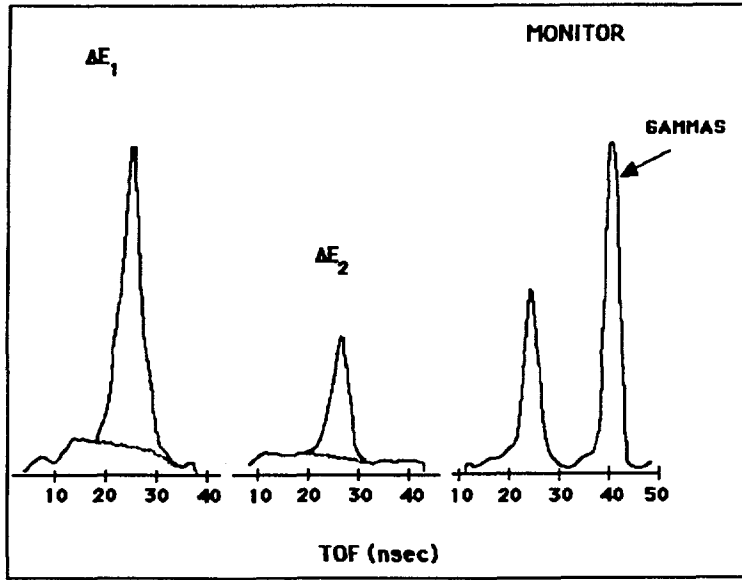


Fig. 6.- Typical TOF neutron spectra observed for the total cross section measurements. Full (dotted) lines correspond to target in (out).

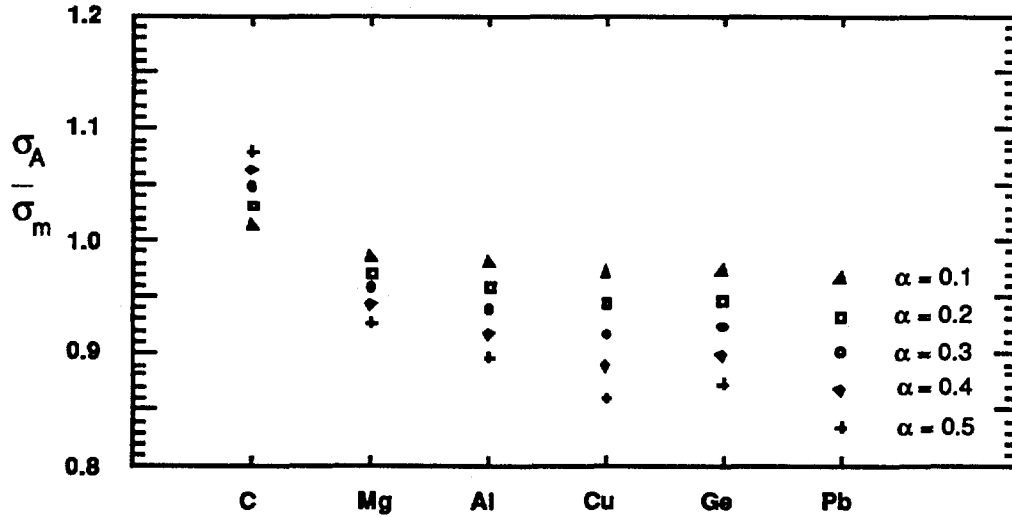


Fig. 7.- Correction ratio for wrap around low energy neutrons. See text.

A consideration based on the cross section for the above reactions and backing target dimensions allowed us to estimate that the intensity of the LEN is about 10% of that of the high energy neutron peak. This results in a correction of less than 4% to the measured cross section. The intensities of both neutron groups are related by a constant α which depends on the geometrical configuration and on the group energies. Then, the cross section for the fast group can be obtained from

$$\sigma = \frac{-1}{NL} \ln \{ e^{-\sigma_m NL} + \alpha (e^{-\sigma_m NL} - e^{-\sigma_B NL}) \} ,$$

where σ_m is the "measured" (low +fast) cross section and σ_B is the total cross section for the low energy group.

In our case, the group of LEN has a maximum energy of about 5 MeV. Values of total neutron cross sections at 5 MeV for the elements used in this work can be taken from the literature.⁶

In order to assess the importance of α , we have formed the ratio of σ_A to σ_m for different values of α in the range from 0.1 to 0.5. These ratios are shown in fig. 7 for the six elements of this work and for 19.8 MeV. The behavior is similar at 17.6 MeV. It is seen that for $\alpha = 0.1$ the largest correction is less than 4%.

Results

Final results for the total cross section measurements are given in Table II. The major uncertainties correspond to statistics, target purity and correction for wrap around neutrons.

Table II. Total cross section for C, Mg, Al, Cu, Ge and Pb measured at 17.6 and 19.8 MeV.

Element	17.6 MeV σ_T (b)	19.8 MeV σ_T (b)
C	1.43 ± 0.07	1.39 ± 0.07
Mg	1.71 ± 0.08	1.63 ± 0.08
Al	1.77 ± 0.09	1.65 ± 0.08
Cu	2.76 ± 0.13	2.61 ± 0.10
Ge	2.98 ± 0.14	2.77 ± 0.13
Pb	5.31 ± 0.26	6.02 ± 0.29

For each of these elements, except Ge, there are several previous measurements in this energy region,^[6] with a rather large dispersion range. All our total cross section results lie within the range determined by the previous measurements.^[6]

In fig. 8 we compare our results for Pb with previous data^[7-10] and with an optical model prediction, finding good agreement in both cases. The Ohio^[11] potential was chosen because of its global character. The same potential was used in the other elements, finding good agreement with the experimental values, except in the cases of C and Cu, where predictions are about 5% above the average.

In fig. 9 we compare our results for Ge with the single data available^[10] and with the Ohio optical model,^[11] observing good agreement.

In figs. 10 and 11 we show the distribution of these new results and older data for C, Mg, Al and Cu in the energy region from 15 to 25 MeV.^{[7-10], [12-28]} The experimental data quoted has been extracted from ref. ^[6].

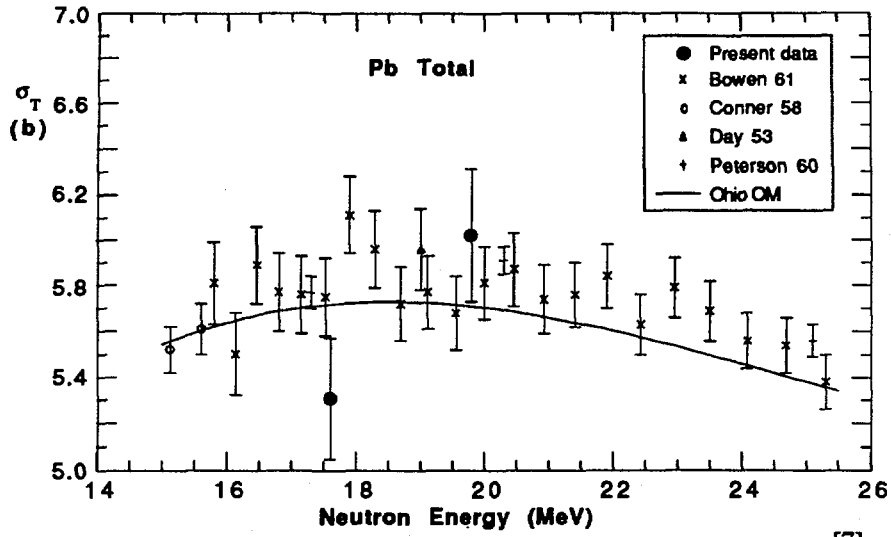


Fig. 8.- Total cross section results for Pb. The other data are from Bowen 61,^[7] Conner 58,^[8] Day 53,^[9] and Peterson 60.^[10] The curve is the optical model potential prediction of Rapaport et al.^[11]

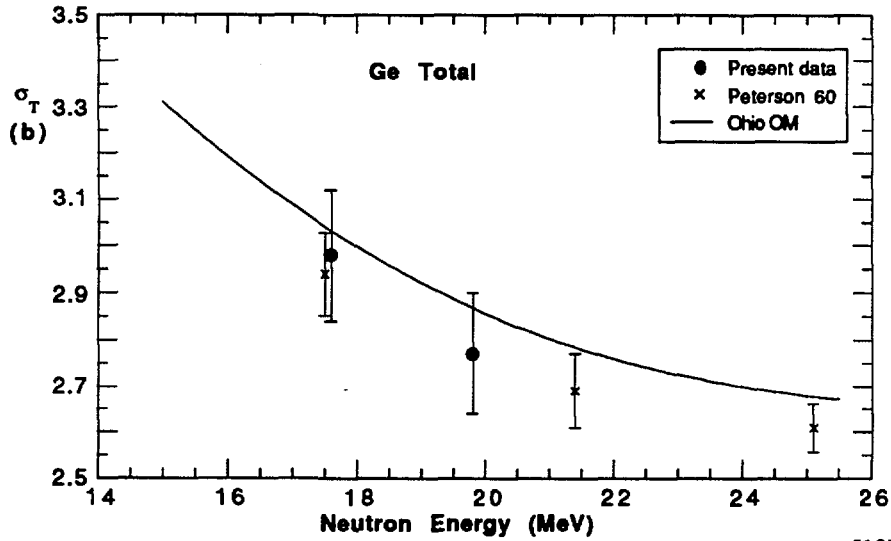


Fig. 9.- Total cross section results for Ge. The other data are from Peterson 60.^[10] The curve is the optical model prediction of Rapaport et al.^[11]

Non elastic measurements

The general set up for non elastic measurements is the same as the one described before. [29-31]

The experimental set up and electronic circuitry remains essentially the same, but for the replacement of detector ΔE_2 by a rather large liquid scintillator detector NE-224, which is placed right behind the target (fig. 12). This large detector fulfills the experimental condition to capture the most of the forward elastic scattered neutrons. Preliminary studies show that this condition is better satisfy at our energies for high Z targets.

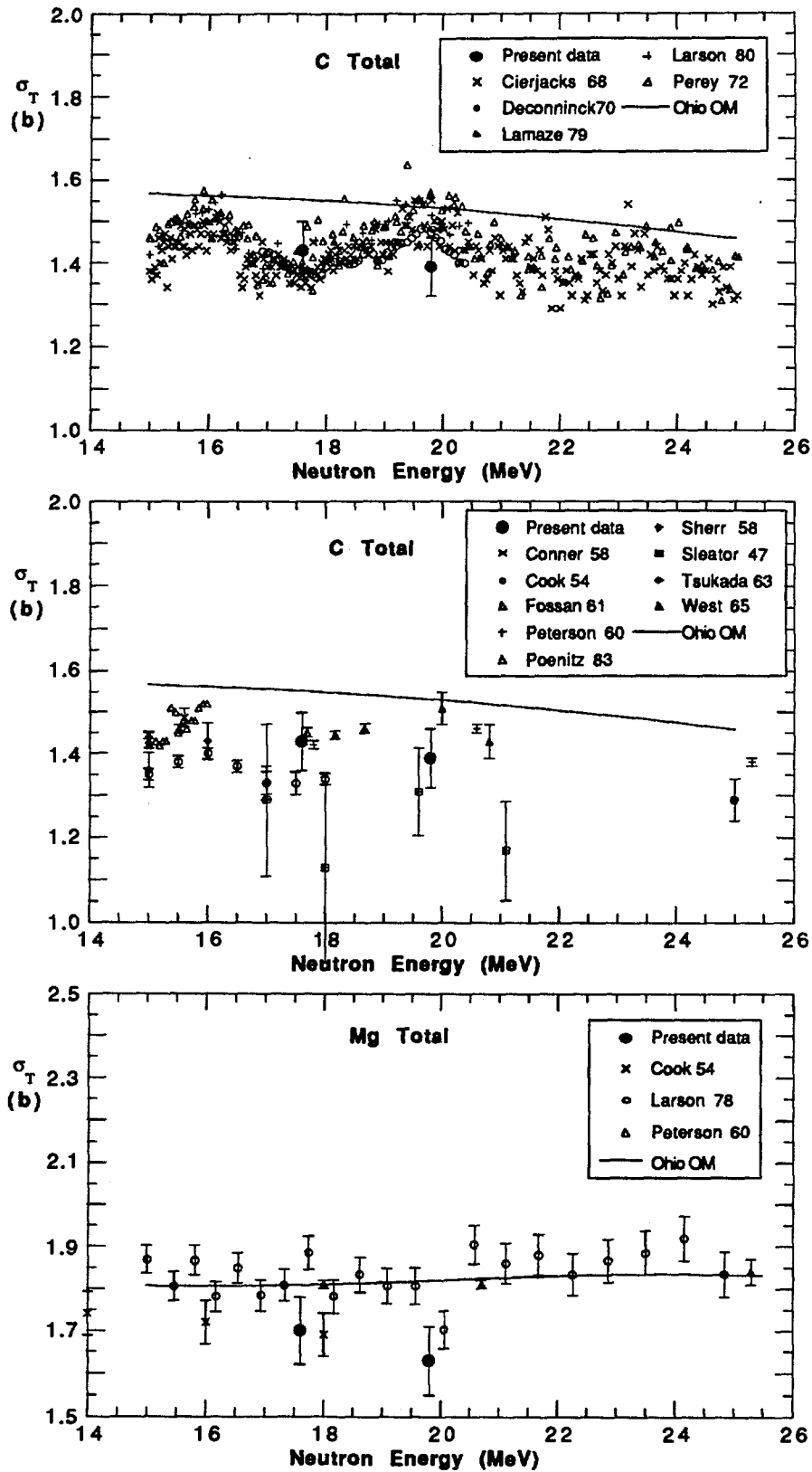


Fig. 10.- Total cross section results for C and Mg. Error bars in some of the data in the top figure have been suppressed for clarity. Other data from [8,10,15-20, 22-23, 25-28].

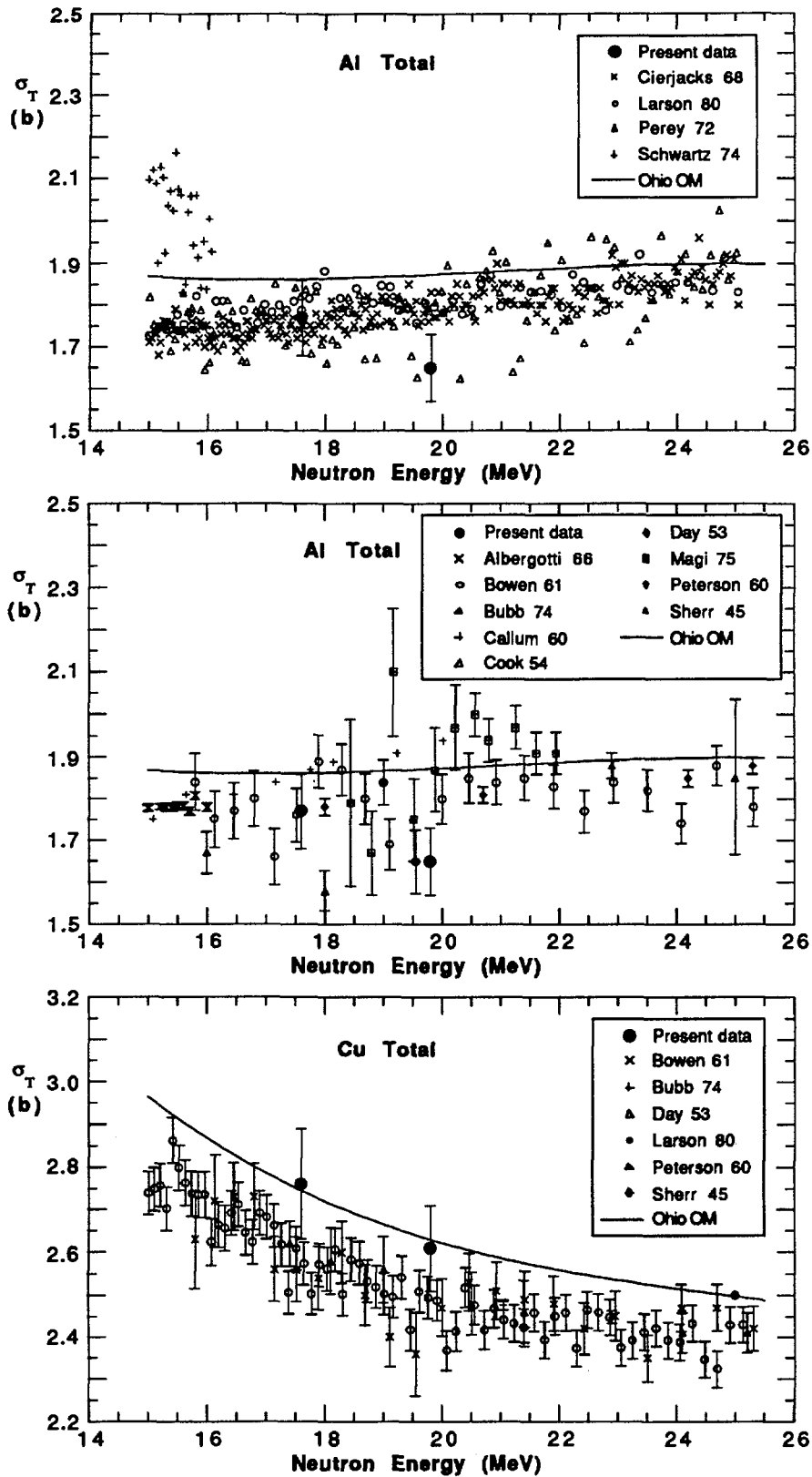


Fig. 11.- Total cross section results for Al and Cu. Error bars in some of the data in the top figure have been suppressed for clarity. Other data from [7,9,10,12-16,20-22,24,25].

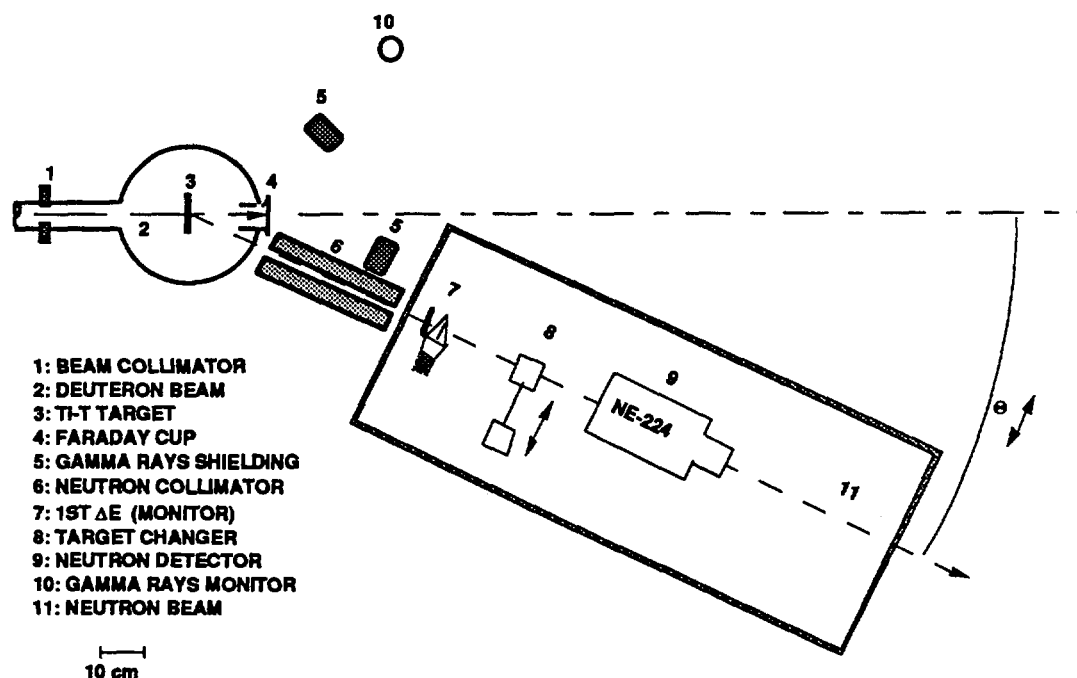


Fig. 12.- Neutron production area and experimental set-up for the non elastic cross section measurements.

Summary

We have described a flexible facility with sounding potential for neutron research in the rather little explored energy region 15-22 MeV. The results presented for total cross sections have shown the reliability of the facility to perform fast neutron measurements. Our results agree with the numerous previous measurements on C, Mg, Al, Cu and Pb. In particular, the Ge results add to the scarce data on this important element and these results may contribute to obtain a better estimation on the damage by fast neutrons in Ge detectors and other devices. Measurements on total non-elastic cross sections will follow, and studies on (n,charged particle) are being considered.

Acknowledgements

We thank Mr. L. O. Figueroa and Mr. R.L. Vallejos for their collaboration during the different stages of this work and Mr. H.O. Riquelme for the skillful operation of the cyclotron. In the development of this experimental facility, the support of the Departamento Técnico de Investigación, Universidad de Chile, and of the Nuclear Data Center, IAEA are gratefully acknowledged. JRM recognizes the kind hospitality of the Crocker Nuclear Laboratory, University of California at Davis, during the final writing of this paper and the travel grant of Fundación Andes. JLR acknowledges PNUD-UNESCO for travel support, the Departamento de Asuntos Internacionales, Universidad de Chile for their hospitality and the National Science Foundation, grant 8722008.

References

- [1] R.C. Haight, UCRL-79453, Lawrence Livermore Laboratory, Livermore, California , U.S.A., 1977.
- [2] WRENDAL, INDC, IAEA, 1986.
- [3] J.A. Jungerman, N.F. Peek and C.G. Patten, Nucl. Inst. and Meth. **18**, 120 (1962) .
- [4] J. R. Morales, J.L. Romero and M.E. Brandan, Nucl.Instrum.&Meth.**119**, 91(1974).
- [5] H. Massmann, Lic. Thesis, U. de Chile (1973) (unpublished).
- [6] V. McLane, C.L. Dunford and P.F. Rose, *Neutron Cross Sections*, National Nuclear Data Center, Brookhaven National Laboratory, U.S.A., vol. 2, 1988. The experimental data has been extracted from the CSISRS compilation, National Nuclear Data Center, Brookhaven National Laboratory, U.S.A. , Nov 1989.
- [7] P.H.Bowen, J.P.Scanlon, G.H.Stafford, J.J.Thresher, P.E.Hodgson, Nucl. Phys. **22**, 640 (1961).
- [8] J.P.Conner, Phys. Rev. **109**, 1268 (1958).
- [9] R.B.Day, R.L.Henkel, Phys. Rev. **92**, 358 (1953).
- [10] J.M.Peterson, A.Bratenahl, J.P.Stoering, Phys. Rev. **120**, 521 (1960).
- [11] J. Rapaport, W. Kulkarni and R. W. Finlay, Nucl. Phys. **A330**, 15 (1974).
- [12] J.C.Albergotti,J.M.Ferguson, Nucl. Phys. **82**, 652 (1966).
- [13] I.F.Bubb,S.N.Bunker,M.Jain,J.W.Leonard,A.Mc IlwainL, K. I. Roulston , K.G. Standing, D.O.Wells,B.G.Whitmore, Can. Journ. Phys. **52**, 648 (1974).
- [14] G.J.Mc Callum,G.S.Mani,A.T.G.Ferguson, Nucl. Phys. **16**, 313 (1960).
- [15] S.Cierjacks, P.Forti, D.Kopsch, L.Kropp, J.Nebe, H.Unseld, Kernforschungszentrum Karlsruhe Report, KFK-1000 (1968).
- [16] C.F.Cook,T.W.Bonner, Phys. Rev. **94**, 651 (1954).
- [17] G.Deconninck, J.P.Meulders, Phys. Rev. **C1**, 1326 (1970).
- [18] D.B.Fossan,R.L.Walter,W.E.Wilson,H.H.Barschall, Phys. Rev. **123**, 209 (1961).
- [19] G.P.Lamaze,J.D.Kellie,R.B.Schwartz, National Bureau Standards, 1979. Data extracted from ref. [6] .
- [20] D.C.Larson,J.A.Harvey,N.W.Hill, Oak Ridge National Laboratory Report, ORNL-5787 (1980).
- [21] R.Magi Ortega Degree Thesis, Universidad Veracruzana, Jalapa, Facultad de Ciencias, Mexico (1975).
- [22] F.G.Perey,T.A.Love,W.E.Kinney, Oak Ridge National Laboratory Report, ORNL-4823 (1972).
- [23] W.P.Poenitz,J.F.Whalen, Argonne National Laboratory Report, ANL-NDM-80 (1983).
- [24] R.B.Schwartz,R.A.Schrack,H.T.Heaton, National Bureau Standards Report, NBS-MONO-138 (1974).

- [25] R.Sherr, Phys. Rev. **68**, 240 (1945).
- [26] W.Sleator, Phys. Rev. **72**, 207 (1947).
- [27] K.Tsukada, Y.C.Hsu, Argonne National Laboratory Report, ANL-NDM-80 (1983).
- [28] M.L.West II,C.M.Jones,H.B.Willard, Oak Ridge National Laboratory Report, ORNL-3778 (1965).
- [29] F. P.Brady, J. L. Romero, C. I. Zanelli, M. L. Johnson, G. A. Needham, J. L. Ullmann, P. P. Urone and D. L. Johnson, Nucl. Inst. and Meth. **178**, 427 (1980).
- [30] C. I. Zanelli, P. P. Urone, J. L. Romero, F. P.Brady, M. L. Johnson, G. A. Needham, J. L. Ullmann and D. L. Johnson, Phys. Rev. **C23**, 1015 (1981).
- [31] J. R. Morales, Report to the IAEA, 1983.